THE JOURNAL OF PHYSICAL CHEMISTRY Letters

pubs.acs.org/JPCL Letter

Synthesis of Superconducting Cobalt Trihydride

Miriam Peña-Alvarez,* Bin Li, Liam C. Kelsall, Jack Binns, Philip Dalladay-Simpson, Andreas Hermann, Ross T. Howie, and Eugene Gregoryanz*

Cite This: J. Phys. Chem. Lett. 2020, 11, 6420−6425 Read Online

ACCESS | Metrics & More | Article Recommendations | Supporting Information

ABSTRACT: The Co−H system has been investigated through high-pressure, high-temperature X-ray diffraction experiments combined with first-principles calculations. On compression of elemental cobalt in a hydrogen medium, we observe face-centered cubic cobalt hydride (CoH) and cobalt dihydride (CoH_2) above 33 GPa. Laser heating CoH_2 in a hydrogen matrix at 75 GPa to temperatures in excess of ∼800 K produces cobalt trihydride (CoH_3) which adopts a primitive structure. Density functional theory calculations support the stability of CoH_3. This phase is predicted to be thermodynamically stable at pressures above 18 GPa and to be a superconductor below 23 K. Theory predicts that this phase remains dynamically stable upon decompression above 11 GPa where it has a maximum T_c of 30 K.

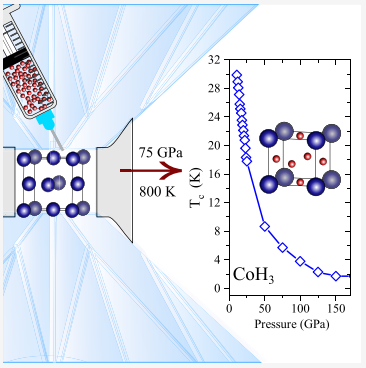

The physical properties of a host metal can be profoundly altered by the presence of hydrogen. It has been predicted that metallic structures that host high density hydrogen could exhibit novel properties such as high-temperature superconductivity.[1] The potentials of these materials are exemplified by the recent high-temperature superconductivity experimentally observed in rare-earth hydrides.[2,3] Prior to these findings, superconductivity was also proposed to emerge in transition metal hydrides (TMH).[4−6]

The transition metals are good electron donors, as they tend to donate their two external s^2 electrons, thus stabilizing the H^- anion over molecular hydrogen. Under moderate pressures, almost all transition metals form monohydride compounds.[7−9] Platinum, for example, is observed to form two hexagonal monohydride variants, PtH-I and PtH-II, at pressures above 27 GPa.[10] *Ab initio* calculations initially predicted PtH-II to be a superconductor, with a critical temperature, T_c, below 17 K at 90 GPa; however, with the inclusion of anharmonic effects, the T_c was substantially reduced to <1 K.[5,10,11] Recent electrical measurements found that at 30 GPa, PtH-II has a T_c of 7 K, which decreased on further compression.[12] Through a combination of high pressure and/or high temperature, TMH with more unusual stochiometries become energetically competitive.[13−22] Iron exhibits several polyhydride species, of which FeH_5 ($I4/mmm$), synthesized at 120 GPa and temperatures >1500 K, is the most hydrogen-rich and possesses a unique layered structure.[23] Potential superconductivity in FeH_5 has been a subject of debate, with two theoretical works predicting remarkably high T_c values ranging between 46 and 51 K and, conversely, another computational study finding no evidence of superconductivity.[24−26] However, the latter study did suggest that trihydrides heavier than FeH_3, with a cubic $Pm\bar{3}m$ structural type, could facilitate superconductivity through the addition of d electrons to the hybrid 3d electron shell of the metal−hydrogen band.[26]

Cobalt is a prime transition metal candidate to also exhibit a trihydride form, being positioned in the same group as iridium and period neighbor iron, both of which form cubic trihydrides.[14,23] Indeed, a recent theoretical study predicted the formation of CoH_3 above 30 GPa sharing the same $Pm\bar{3}m$ structure as both FeH_3 and IrH_3.[27] However, both these studies and a further computational work predict CoH_3 to have a T_c below 1 K at pressures above 150 GPa.[26,27] Experimentally, the synthesis of CoH_3 has remained elusive, with only the formation of face-centered cubic (fcc) CoH above 4 GPa[9] and the stepwise transition to CoH_2 above 45 GPa.[20]

Here, we demonstrate the synthesis of cobalt trihydride in a laser-heated diamond-anvil cell through a series of synchrotron X-ray diffraction experiments. On compression, we observe formation of the known CoH and CoH_2, which we find to coexist to at least 75 GPa. Laser heating CoH and CoH_2 in a hydrogen matrix at pressures and temperatures above 75 GPa and 700 K leads to the complete transformation of the sample, identified by new diffraction peaks. We identify the new

Received: June 10, 2020
Accepted: July 13, 2020
Published: July 13, 2020

https://dx.doi.org/10.1021/acs.jpclett.0c01807
J. Phys. Chem. Lett. 2020, 11, 6420−6425

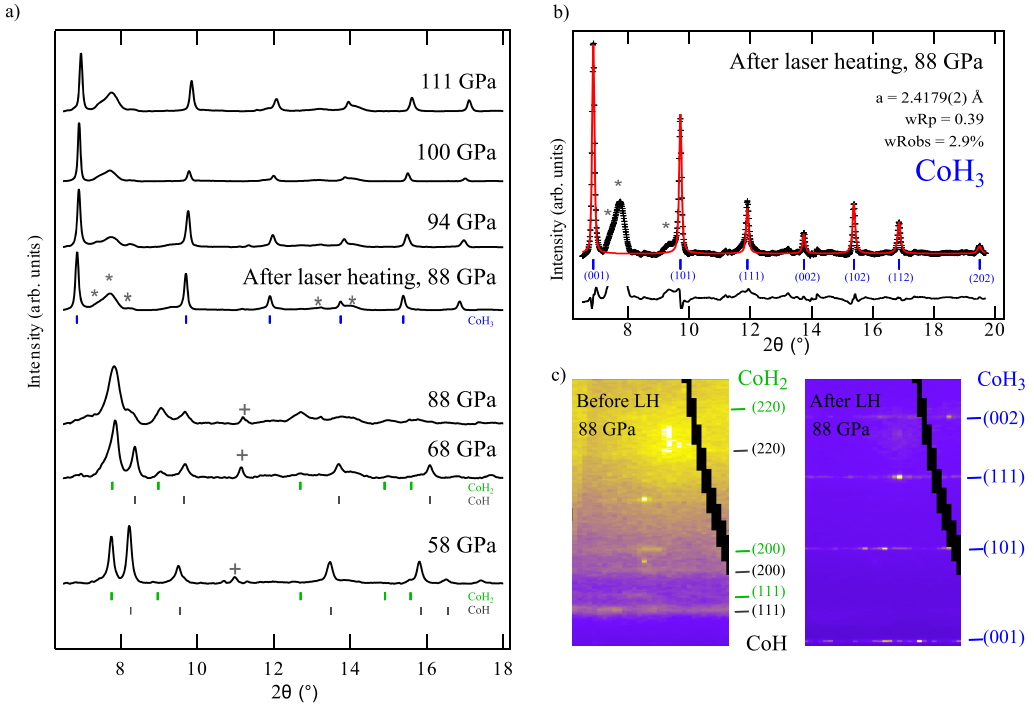

Figure 1. (a) High-pressure X-ray diffraction patterns (λ = 0.2895 Å) taken on compression to 111 GPa. Laser heating at 88 GPa yields the synthesis of $Pm\bar{3}m$ cobalt trihydride. Asterisks correspond to Re and ReH, while crosses correspond to W. (b) Rietveld refinement fit of CoH_3 structures, unfitted peaks marked by * correspond to ReH and Re. Refinement parameters are wRp = 0.39 and wR_{obs} = 2.9. (c) Diffraction plates of the sample at 88 GPa before (left) and after (right) laser heating. In all panels, tick marks indicate the reflections of CoH (gray), CoH_2 (green), and CoH_3 (blue).

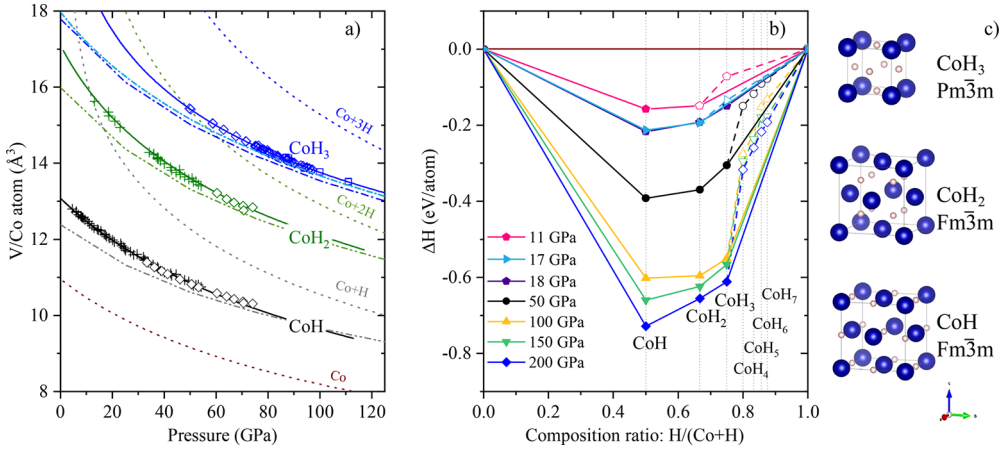

Figure 2. (a) Volume per Co atom for Co−H compounds. Diamond and square symbols correspond to measurements from two experimental runs, while crosses represent data taken from Wang et al.[20] Solid lines correspond to the experimental equation of states (EOS) calculated using data from this work and Wang et al.[20] Dashed dotted lines were calculated through DFT using ultrasoft pseudopotentials (QuantumESPRESSO code). For CoH_3 the light blue dashed−dotted line was calculated with VASP, using hard PAW pseudopotentials and the optB88-vdW dispersion-corrected functional. Dotted lines represent the EOS derived from the atomic volumes of Co and H.[28,29] (b) Convex hull construction for CoH_x compounds at a sequence of pressures. Empty (filled) symbols denote metastable (stable) phases. (c) Crystal structures of cobalt polyhydrides, CoH ($Fm\bar{3}m$), CoH_2 ($Fm\bar{3}m$) and CoH_3 ($Pm\bar{3}m$). Co atoms are represented by blue spheres, and H atoms are represented by pink spheres.

compound as CoH_3 and find it to be isostructural to FeH_3, with Co atoms occupying the vertices of a primitive cubic unit cell and H atoms occupying the vacant face centers.[15] Total energy and electron−phonon calculations reveal that CoH_3 remains energetically stable down to 18 GPa, at which pressure it exhibits superconductivity with a T_c of 23 K.

After gas loading at 0.2 GPa, mixtures of Co and H_2 were compressed to 33 GPa. After 1 week at this pressure, X-ray diffraction patterns reveal the synthesis of both CoH and CoH_2 compounds, in agreement with previous work.[20] CoH has space group symmetry $Fm\bar{3}m$, with unit-cell length a = 3.4849(7) Å (at 60 GPa), while CoH_2 has unit cell length a = 3.7533(8) Å (at 60 GPa) within the same group. Interestingly, CoH_2 is not isostructural to FeH_2, which adopts a tetragonal $I4/mmm$ structure,[15] but instead adopts the same structure as RhH_2 at 14 GPa.[13] We find that both CoH and CoH_2 coexist

https://dx.doi.org/10.1021/acs.jpclett.0c01807
J. Phys. Chem. Lett. 2020, 11, 6420−6425

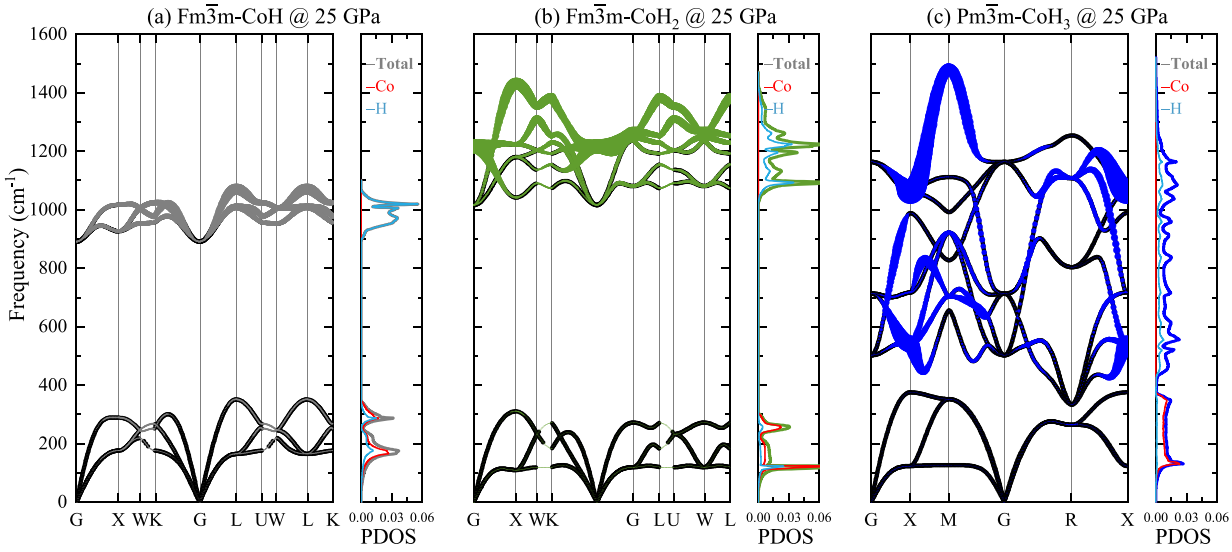

Figure 3. Phonon dispersion curves and projected phonon density of states at at 25 GPa for (a) CoH, (b) CoH_2, and (c) CoH_3. The phonon dispersions $\omega_\nu(\mathbf{q})$ for each phonon mode ν at momentum space point $\mathbf{q}$ are drawn as circles with radii proportional to the magnitude of the electron−phonon line widths $\gamma_{\mathbf{q}\,\nu}$.

up to pressures of 88 GPa (see Figure 1a), with no indication of further hydrogenation. We also do not observe a transition on compression to tetragonal ($I4/mmm$) CoH_2, which was predicted to become energetically favorable above 42 GPa.[27]

The laser heating of metals in a high-pressure hydrogen environment has been a successful synthetic tool in yielding hydrogen-rich metal hydrides[3,17,30,31] and was utilized here to explore the synthesis of cobalt polyhydride species. Samples of CoH/CoH_2 and H_2 were compressed to pressures of 75 and 88 GPa and held here for 24 and 12 h, respectively, displaying no time-induced transformation. These samples were then laser heated to approximately about 800 K (Figure S1 and see Experimental and Theoretical Methods in the Supporting Information for further details). Upon quenching of the sample, we see the disappearance of the diffraction lines attributed to CoH/CoH_2, which are supplanted by new diffraction peaks (see Figures 1a,c and S1[32]). All of the new diffraction peaks can be indexed with a simple cubic unit cell ($Pm\bar{3}m$) with lattice parameter a = 2.4358(2) Å at 75 GPa. Rietveld refinements of this structure (Figure 1b) show Co atoms to be on the vertexes of the unit cell, with final agreement factors of wRp = 0.39 and a wR_{obs} = 2.9. Samples were compressed up to 111 GPa, the highest pressure reached in this study, and subsequently decompressed down to 52 GPa (below which the sample was lost because of anvil failure) to determine the equation of state (EOS) and evaluate the stability of the compound. The volume per Co atom as a function of pressure of CoH, CoH_2, and the synthesized product was fitted with third-order Birch−Murnaghan $P-V$ EOS's (see Figure 2a) with the fit parameters shown in Table S1. The experimentally determined EOS gives volumes greater than Co + 2H. The determined structure also matches that which was previously predicted for CoH_3[27] and is isostructural to FeH_3,[15] synthesized through similar methods.

We have performed our own variable-composition structure search to find energetically stable structures in the Co−H system up to 400 GPa using the evolutionary crystal structure prediction method USPEX package and the particle swarm optimization method as implemented in the CALYPSO code (Figures S2−S4).[33−37] Through enthalpy calculations for the most stable structures, we find CoH_3 to adopt a $Pm\bar{3}m$ unit cell identical to FeH_3[15,38] and IrH_3,[14] with the H atoms occupying the 3c site $(0, \frac{1}{2}, \frac{1}{2})$. This, together with the computationally determined EOS, is in good agreement with experiments. CoH_3 is on the convex hull above 18 GPa; however, experimentally we see only CoH and CoH_2, which we attribute to kinetics barriers. CoH and CoH_2 have the highest formation enthalpies, 0.602 and 0.596 eV per atom, respectively, at 100 GPa (see Figure 2) and also share the same fcc-Co sub lattice. Pure Co adopts a hcp phase at pressures below 105 GPa, above which it transforms to fcc-Co.[29] So although fcc-Co is not the ground state at 33−55 GPa, it is likely there is a low energy barrier[39] to form metastable fcc-Co, which can then be filled with hydrogen to form CoH and/or CoH_2. Experimentally, both compounds can be formed on compression alone, with laser heating accelerating the process.[20]

CoH_3, however, is very different, because it has a simple cubic Co sub lattice. Because it is not close-packed, a major rearrangement of the Co lattice is required to allow the formation of CoH_3. Neither low pressure and high temperature or long times at pressures below 50 GPa are sufficient to initiate the CoH_3 formation,[20] requiring pressures above 75 GPa and laser heating to trigger the CoH_3 synthesis. In agreement with the convex hull calculations, and Gibbs' phase rule, only CoH_3 is formed after the laser heating in an H_2 rich environment. Our DFT calculations also find an unreported structural transition in CoH_2 above 275 GPa to a tetragonal $P4/nmm$ phase (Figure S4).

Recent theoretical work anticipated that transition metal trihydrides isostructural to FeH_3 but with heavier elements, like Co, would be candidates to undergo superconducting transitions.[26] Our DFT calculations of the electronic structure and electronic bands demonstrate metallicity of the three hydrides at all pressures throughout their stability ranges (see Figures S5−S8). At the lowest pressure, the electronic density of states (DOS) of CoH_3 (see Figure S5) has important

https://dx.doi.org/10.1021/acs.jpclett.0c01807
J. Phys. Chem. Lett. 2020, 11, 6420−6425

contributions from hydrogen orbitals around the Fermi level, indicative that it could exhibit superconductivity.

In Figure 3 we show the calculated phonon dispersion curves and projected phonon density of states (PDOS) for the low-pressure phases of CoH, CoH_2, and CoH_3 at 25 GPa (see Figures S9−S12 for higher- and lower-pressure results). Phonon structures of all the hydrides depict no imaginary frequencies along the high-symmetry k path, which demonstrates their dynamical stability. For $Fm\bar{3}m$-CoH, as shown in Figure 3a, a phonon gap between 400 and 900 cm^{-1} divides the spectrum into two regions: the low-frequency acoustic branches and high-frequency optical branches. The optical modes are associated with almost exclusive motion of H atoms, whereas the acoustic modes are associated with the concerted motions of both Co and H atoms. From Figure 3b, CoH_2 has a similar gapped phonon spectrum compared to CoH, but with higher optical frequency branches up to 1400 cm^{-1} in the hydrogenic sublattice. In CoH_3, there is a big change in the phonon dispersion and PDOS. The phonon gap has shrunk, and the larger number of optical branches occupies a much wider frequency region. From CoH to CoH_3, the magnitude of the electron−phonon line-widths increases with the higher hydrogen content, which may lead to a higher zone-averaged electron−phonon coupling parameter (EPC) and superconducting critical temperature, T_c.

We estimate the EPC and T_c using the McMillan−Allen−Dynes formula[40−42]

$$T_c = \frac{\omega_{ln}}{1.2}\exp\left[-\frac{1.04(1+\lambda)}{\lambda - \mu^*(1+0.62\lambda)}\right]$$

where ω_{ln} is the logarithmically averaged phonon frequency, and taking the Coulomb parameter as $\mu^* = 0.1$. The EPC λ and T_c are plotted in Figure 4 as a function of pressure. For CoH and CoH_2, the calculated λ values are below ~0.45 in the studied pressure range. Such weak EPC values result in T_c below 2 K. However, as seen in Figure 4, CoH_3 shows a different and remarkable trend with λ significantly increased with decreasing pressure, which in turn leads to a rapid T_c increase upon decompression, reaching a predicted maximum of 30 K at 11 GPa.

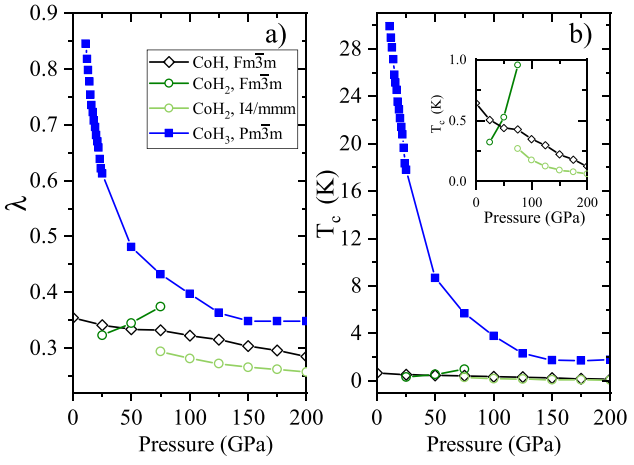

Figure 4. (a) Electron−phonon coupling constant λ for the calculated favored cobalt hydrides phases as a function of pressure. (b) Critical temperature, T_c, for CoH, CoH_2, and CoH_3 as a function of pressure. Inset shows T_c as a function of pressure between 0 and 1 K. In all panels, CoH is represented as black diamonds, CoH_2 as green circles, and CoH_3 as blue squares.

There are some quantitative differences between our results and those obtained in previous calculations.[27] For CoH_3 at 200 GPa we obtain $\lambda = 0.35$ and $T_c = 2$ K, while Wang et al.[27] obtain $\lambda = 0.19$ and $T_c \approx 0$ K. We have repeated our calculations with parameters very similar to those used by Wang et al. (see Figures S13−S23) and reproduce the EPC and T_c data (Figure S23, $\lambda = 0.21$ and $T_c = 4$ mK). We postulate that the choice of pseudopotential—norm-conserving (NC) in Wang et al.[27] and ultrasoft (US) here—is the source of the quantitative differences we see. The US pseudopotentials are better suited than the NC to describe the EOS of pure Co and H[43] but give very similar EOS results for CoH_3; both also agree with VASP calculations using the PAW method (see Figure S13 in the Supporting Information). The choice of pseudopotential has a larger effect on phonon properties than on electronic properties; Figure S14 in the Supporting Information compares them to VASP results. Nonetheless, using either approach, the EPC and T_c share the same trend upon compression, but on different absolute scales (see Figure S23); with the NC pseudopotentials, the T_c of CoH_3 is predicted to reach 15 K at 13 GPa. The US pseudopotentials give the same value if the screened Coulomb interaction μ^* would be increased to 0.18. These quantitative uncertainties might be best resolved by using more sophisticated theoretical approaches such as directly solving the Eliashberg equation or the superconducting DFT method.[44,45]

The strong negative pressure dependence of T_c in CoH_3 at these low pressures can be explained by the hardening of the phonon frequencies leading to a weakening of EPC λ. As shown in Figures 3 and S9−S12, when the pressure increases from 10 to 300 GPa, the maximal frequencies of optical phonon branches for CoH_3 harden from 1500 to 2400 cm^{-1}, while the DOS $N(0)$ (see Figures S6−S8) and magnitude of electron−phonon line widths $\gamma_{\nu q}$ remain almost unchanged. A similar trend in T_c was experimentally observed in PtH-II, from 7 K at 30 GPa to 5 K at 40 GPa.[12]

In our experimental runs, diamond failure on decompression prevented us from studying the stability of CoH_3 at pressures lower than 52 GPa. At 52 GPa, we predict CoH_3 to have T_c of 8 K, which could increase to 30 K at 11 GPa. We speculate that because of the large stability range predicted for CoH_3 (Figure S1), that low temperature could maintain the stability of CoH_3 down to it is maximal T_c conditions, and such behavior should be explored in future studies.

The predicted superconducting character of CoH_3 proves that TMH_3 samples heavier than FeH_3 do facilitate more efficient electron−phonon coupling. We have demonstrated the formation of CoH_3 synthesized at 75 GPa and stable in decompression to at least 52 GPa. CoH_3 adopts a cubic $Pm\bar{3}m$ structure which is very stable both in compression up to 111 GPa and in decompression down to 52 GPa. Our DFT results predict that this structure should be superconducting with a T_c which increased with decreasing pressure, reporting a maximum of 30 K at 11 GPa. These results give an indication that superconductivity could also be observed in metal hydrides at low-pressure conditions.

https://dx.doi.org/10.1021/acs.jpclett.0c01807
J. Phys. Chem. Lett. 2020, 11, 6420−6425

■ ASSOCIATED CONTENT

Supporting Information

The Supporting Information is available free of charge at https://pubs.acs.org/doi/10.1021/acs.jpclett.0c01807.

Experimental and theoretical methods; equation of state parameters, electronic and phonon band structures, and experimental and calculated unit-cell parameters (PDF)

■ AUTHOR INFORMATION

Corresponding Authors

Miriam Peña-Alvarez − *Centre for Science at Extreme Conditions & The School of Physics and Astronomy, The University of Edinburgh, Edinburgh, U.K.;* orcid.org/0000-0001-7056-7158; Email: mpenaal@ed.ac.uk

Eugene Gregoryanz − *Center for High Pressure Science & Technology Advanced Research, 1690 Cailun Road, Shanghai 201203, China; Centre for Science at Extreme Conditions & The School of Physics and Astronomy, The University of Edinburgh, Edinburgh, U.K.;* Email: e.gregoryanz@ed.ac.uk

Authors

Bin Li − *New Energy Technology Engineering Laboratory of Jiangsu Province and School of Science, Nanjing University of Posts and Telecommunications, Nanjing 210023, China; National Laboratory of Solid State Microstructures, Nanjing University, Nanjing 210093, China;* orcid.org/0000-0002-6392-4185

Liam C. Kelsall − *Centre for Science at Extreme Conditions & The School of Physics and Astronomy, The University of Edinburgh, Edinburgh, U.K.*

Jack Binns − *Center for High Pressure Science & Technology Advanced Research, 1690 Cailun Road, Shanghai 201203, China;* orcid.org/0000-0001-5421-6841

Philip Dalladay-Simpson − *Center for High Pressure Science & Technology Advanced Research, 1690 Cailun Road, Shanghai 201203, China*

Andreas Hermann − *Centre for Science at Extreme Conditions & The School of Physics and Astronomy, The University of Edinburgh, Edinburgh, U.K.;* orcid.org/0000-0002-8971-3933

Ross T. Howie − *Center for High Pressure Science & Technology Advanced Research, 1690 Cailun Road, Shanghai 201203, China*

Complete contact information is available at: https://pubs.acs.org/10.1021/acs.jpclett.0c01807

Notes

The authors declare no competing financial interest.

■ ACKNOWLEDGMENTS

M.P.-A. acknowledges the support of the European Research Council (ERC) Grant "Hecate" reference No. 695527 held by Prof. G. J. Ackland. R.T.H. would like to acknowledge the support of the National Science Foundation of China (Grant No. 11974034). Portions of this work were performed at GeoSoilEnviroCARS (The University of Chicago, Sector 13), Advanced Photon Source (APS), Argonne National Laboratory. GeoSoilEnviroCARS is supported by the National Science Foundation - Earth Sciences (EAR - 1634415) and Department of Energy - GeoSciences (DE-FG02-94ER14466). We acknowledge DESY (Hamburgh, German) a member of the Helmholtz Association HGF, for the provision of experimental facilites. Parts of this research were carried out at PETRA-III, and we thank H.-P. Liermann and N. Giordiano for assistance in using beamline P02.2 (I-20191366). This research used resources of the Advanced Photon Source, a U.S. Department of Energy (DOE) Office of Science User Facility operated for the DOE Office of Science by Argonne National Laboratory under Contract No. DE-AC02-06CH11357. Computational resources provided by the UK's National Supercomputer Service through the UK Car−Parrinello consortium (EP/P022561/1) and project ID d56 "Planetary Interiors" and by the UK Materials and Molecular Modelling Hub (EP/P020194) are gratefully acknowledged.

■ REFERENCES

(1) Ashcroft, N. Hydrogen dominant metallic alloys: high temperature superconductors? *Phys. Rev. Lett.* **2004**, *92*, 187002.

(2) Drozdov, A.; Kong, P.; Minkov, V.; Besedin, S.; Kuzovnikov, M.; Mozaffari, S.; Balicas, L.; Balakirev, F.; Graf, D.; Prakapenka, V.; et al. Superconductivity at 250 K in lanthanum hydride under high pressures. *Nature* **2019**, *569*, 528.

(3) Somayazulu, M.; Ahart, M.; Mishra, A. K.; Geballe, Z. M.; Baldini, M.; Meng, Y.; Struzhkin, V. V.; Hemley, R. J. Evidence for Superconductivity above 260 K in Lanthanum Superhydride at Megabar Pressures. *Phys. Rev. Lett.* **2019**, *122*, 27001.

(4) Scheler, T.; Degtyareva, O.; Gregoryanz, E. On the effects of high temperature and high pressure on the hydrogen solubility in rhenium. *J. Chem. Phys.* **2011**, *135*, 214501.

(5) Kim, D. Y.; Scheicher, R. H.; Pickard, C. J.; Needs, R.; Ahuja, R. Predicted formation of superconducting platinum-hydride crystals under pressure in the presence of molecular hydrogen. *Phys. Rev. Lett.* **2011**, *107*, 117002.

(6) Gao, G.; Hoffmann, R.; Ashcroft, N. W.; Liu, H.; Bergara, A.; Ma, Y. Theoretical study of the ground-state structures and properties of niobium hydrides under pressure. *Phys. Rev. B: Condens. Matter Mater. Phys.* **2013**, *88*, 184104.

(7) Antonov, V. Phase transformations, crystal and magnetic structures of high-pressure hydrides of d-metals. *J. Alloys Compd.* **2002**, *330*, 110−116.

(8) Baranowski, B. High Pressure Research on Palladium-Hydrogen Systems. *Platinum Metals Review* **1972**, *16*, 10−15.

(9) Kuzovnikov, M.; Tkacz, M. High pressure studies of cobalt−hydrogen system by X-ray diffraction. *J. Alloys Compd.* **2015**, *650*, 884−886.

(10) Scheler, T.; Degtyareva, O.; Marqués, M.; Guillaume, C. L.; Proctor, J. E.; Evans, S.; Gregoryanz, E. Synthesis and properties of platinum hydride. *Phys. Rev. B: Condens. Matter Mater. Phys.* **2011**, *83*, 214106.

(11) Errea, I.; Calandra, M.; Mauri, F. Anharmonic free energies and phonon dispersions from the stochastic self-consistent harmonic approximation: Application to platinum and palladium hydrides. *Phys. Rev. B: Condens. Matter Mater. Phys.* **2014**, *89*, No. 064302.

(12) Matsuoka, T.; Hishida, M.; Kuno, K.; Hirao, N.; Ohishi, Y.; Sasaki, S.; Takahama, K.; Shimizu, K. Superconductivity of platinum hydride. *Phys. Rev. B: Condens. Matter Mater. Phys.* **2019**, *99*, 144511.

(13) Li, B.; Ding, Y.; Kim, D. Y.; Ahuja, R.; Zou, G.; Mao, H.-K. Rhodium dihydride RhH2 with high volumetric hydrogen density. *Proc. Natl. Acad. Sci. U. S. A.* **2011**, *108*, 18618−18621.

(14) Scheler, T.; Marqués, M.; Konôpková, Z.; Guillaume, C. L.; Howie, R. T.; Gregoryanz, E. High-Pressure Synthesis and Characterization of Iridium Trihydride. *Phys. Rev. Lett.* **2013**, *111*, 215503.

(15) Pépin, C. M.; Dewaele, A.; Geneste, G.; Loubeyre, P.; Mezouar, M. New Iron Hydrides under High Pressure. *Phys. Rev. Lett.* **2014**, *113*, 265504.

(16) Liu, G.; Besedin, S.; Irodova, A.; Liu, H.; Gao, G.; Eremets, M.; Wang, X.; Ma, Y. Nb-H system at high pressures and temperatures. *Phys. Rev. B: Condens. Matter Mater. Phys.* **2017**, *95*, 104110.

(17) Binns, J.; Donnelly, M.-E.; Wang, M.; Hermann, A.; Gregoryanz, E.; Dalladay-Simpson, P.; Howie, R. T. Synthesis of Ni

2 H 3 at high temperatures and pressures. *Phys. Rev. B: Condens. Matter Mater. Phys.* **2018**, *98*, 140101.
(18) Ying, J.; Liu, H.; Greenberg, E.; Prakapenka, V. B.; Struzhkin, V. V. Synthesis of new nickel hydrides at high pressure. *Physical Review Materials* **2018**, *2*, No. 085409.
(19) Marizy, A.; Geneste, G.; Loubeyre, P.; Guigue, B.; Garbarino, G. Synthesis of bulk chromium hydrides under pressure of up to 120 GPa. *Phys. Rev. B: Condens. Matter Mater. Phys.* **2018**, *97*, 184103.
(20) Wang, M.; Binns, J.; Donnelly, M.-E.; Peña-Alvarez, M.; Dalladay-Simpson, P.; Howie, R. T. High pressure synthesis and stability of cobalt hydrides. *J. Chem. Phys.* **2018**, *148*, 144310.
(21) Ying, J.; Li, X.; Greenberg, E.; Prakapenka, V. B.; Liu, H.; Struzhkin, V. V. Synthesis and stability of tantalum hydride at high pressures. *Phys. Rev. B: Condens. Matter Mater. Phys.* **2019**, *99*, 224504.
(22) Binns, J.; He, Y.; Donnelly, M.-E.; Peña-Alvarez, M. M.; Wang, M.; Kim, D. Y.; Gregoryanz, E.; Dalladay-Simpson, P.; Howie, R. T. Complex Hydrogen Substructure in Semimetallic RuH_4. *J. Phys. Chem. Lett.* **2020**, *11*, 3390−3395.
(23) Pépin, C.; Geneste, G.; Dewaele, A.; Mezouar, M.; Loubeyre, P. Synthesis of FeH5: A layered structure with atomic hydrogen slabs. *Science* **2017**, *357*, 382−385.
(24) Majumdar, A.; Tse, J. S.; Wu, M.; Yao, Y. Superconductivity in FeH 5. *Phys. Rev. B: Condens. Matter Mater. Phys.* **2017**, *96*, 201107.
(25) Kvashnin, A. G.; Kruglov, I. A.; Semenok, D. V.; Oganov, A. R. Iron superhydrides FeH5 and FeH6: stability, electronic properties, and superconductivity. *J. Phys. Chem. C* **2018**, *122*, 4731−4736.
(26) Heil, C.; Bachelet, G. B.; Boeri, L. Absence of superconductivity in iron polyhydrides at high pressures. *Phys. Rev. B: Condens. Matter Mater. Phys.* **2018**, *97*, 214510.
(27) Wang, L.; Duan, D.; Yu, H.; Xie, H.; Huang, X.; Tian, F.; Liu, B.; Cui, T. High-Pressure Formation of Cobalt Polyhydrides: A First-Principle Study. *Inorg. Chem.* **2018**, *57*, 181−186.
(28) Loubeyre, P.; LeToullec, R.; Hausermann, D.; Hanfland, M.; Hemley, R.; Mao, H.; Finger, L. X-ray diffraction and equation of state of hydrogen at megabar pressures. *Nature* **1996**, *383*, 702.
(29) Yoo, C.; Cynn, H.; Söderlind, P.; Iota, V. New β (fcc)-Cobalt to 210 GPa. *Phys. Rev. Lett.* **2000**, *84*, 4132.
(30) Binns, J.; Peña-Alvarez, M.; Donnelly, M.-E.; Gregoryanz, E.; Howie, R. T.; Dalladay-Simpson, P. Structural Studies on the Cu−H System under Compression. *Engineering* **2019**, *5*, 505−509.
(31) Peña-Alvarez, M.; Binns, J.; Hermann, A.; Kelsall, L. C.; Dalladay-Simpson, P.; Gregoryanz, E.; Howie, R. T. Praseodymium polyhydrides synthesized at high temperatures and pressures. *Phys. Rev. B: Condens. Matter Mater. Phys.* **2019**, *100*, 184109.
(32) See the Supporting Information.
(33) Oganov, A. R.; Glass, C. W. Crystal structure prediction using ab initio evolutionary techniques: Principles and applications. *J. Chem. Phys.* **2006**, *124*, 244704.
(34) Glass, C. W.; Oganov, A. R.; Hansen, N. USPEXEvolutionary crystal structure prediction. *Comput. Phys. Commun.* **2006**, *175*, 713−720.
(35) Bushlanov, P. V.; Blatov, V. A.; Oganov, A. R. Topology-based crystal structure generator. *Comput. Phys. Commun.* **2019**, *236*, 1−7.
(36) Wang, Y.; Lv, J.; Zhu, L.; Ma, Y. Crystal structure prediction via particle-swarm optimization. *Phys. Rev. B: Condens. Matter Mater. Phys.* **2010**, *82*, No. 094116.
(37) Wang, Y.; Lv, J.; Zhu, L.; Ma, Y. CALYPSO: A Method for Crystal Structure Prediction. *Comput. Phys. Commun.* **2012**, *183*, 2063−2070.
(38) Bazhanova, Z. G.; Oganov, A. R.; Gianola, O. Fe−C and Fe−H systems at pressures of the Earth's inner core. *Phys.-Usp.* **2012**, *55*, 489.
(39) Yang, J. X.; Zhao, H. L.; Gong, H. R.; Song, M.; Ren, Q. Q. Proposed mechanism of HCP FCC phase transition in titianium through first principles calculation and experiments. *Sci. Rep.* **2018**, *8*, 1992.
(40) McMillan, L. W. Transition Temperature of Strong-Coupled Superconductors. *Phys. Rev.* **1968**, *167*, 331−344.
(41) Allen, P. B.; Dynes, R. C. Transition temperature of strong-coupled superconductors reanalyzed. *Phys. Rev. B* **1975**, *12*, 905−922.
(42) Li, B.; Miao, Z.; Ti, L.; Liu, S.; Chen, J.; Shi, Z.; Gregoryanz, E. Predicted high-temperature superconductivity in cerium hydrides at high pressures. *J. Appl. Phys.* **2019**, *126*, 235901.
(43) Prandini, G.; Marrazzo, A.; Castelli, I. E.; Mounet, N.; Marzari, N. Precision and efficiency in solid-state pseudopotential calculations. *Computational Materials* **2018**, *4*, 72.
(44) Margine, E. R.; Giustino, F. Anisotropic Migdal-Eliashberg theory using Wannier functions. *Phys. Rev. B: Condens. Matter Mater. Phys.* **2013**, *87*, No. 024505.
(45) Lüders, M.; Marques, M. A. L.; Lathiotakis, N. N.; Floris, A.; Profeta, G.; Fast, L.; Continenza, A.; Massidda, S.; Gross, E. K. U. Ab initio theory of superconductivity. I. Density functional formalism and approximate functionals. *Phys. Rev. B: Condens. Matter Mater. Phys.* **2005**, *72*, No. 024545.

https://dx.doi.org/10.1021/acs.jpclett.0c01807
J. Phys. Chem. Lett. 2020, 11, 6420−6425